DALTON

Organotin-functionalised poly(tetrazoles), including the supramolecular structure of 1,6-(2-$Bu_3SnN_4C)_2(CH_2)_6$

Anna Goodger, Michael Hill, Mary F. Mahon, John McGinley and Kieran C. Molloy *

School of Chemistry, University of Bath, Claverton Down, Bath BA2 7AY, UK

Eight α,ω-bis(triorganostannyltetrazolyl)alkanes, 1,*n*-$(R_3SnN_4C)_2(CH_2)_n$ (*n* = 1,2,4–6; R = Me, Et, Pr^i or Bu) have been synthesised by a cycloaddition method involving SnR_3N_3 and 1,*n*-$(NC)_2(CH_2)_n$. The structure of the compound with R = Bu and *n* = 6 has been determined. It adopts a unique bilayer arrangement incorporating 40- and 58-membered rings which generate channels through the lattice array in all three dimensions.

We have been investigating the structural chemistry of organotin tetrazoles and have reported the synthesis and structural characterisation of the novel bicyclic species **I**.[1,2] The central *trans*-N_2SnC_3 unit in **I** with a near-linear N–Sn–N component is a consistent feature of the structural chemistry of organotin tetrazoles, as we have established both crystallographically and on the basis of Mössbauer spectroscopy.[2,3] Our more recent work [3] has been concerned with organotin species which embody more than one tetrazole unit such as **II**, since such species can form supramolecular arrays based upon the multidentate nature of the tetrazoles and their versatile use of ligating atoms *i.e.* combinations of N^1 and N^2 bonding modes (see **II** for numbering scheme; note that structurally N^1 and N^4 are equivalent, as are N^2 and N^3, thus only N^1 and N^2 are used in the following text to describe the co-ordination of tin with respect to the tetrazole). In this way the *trans*-N_2SnC_3 group provides a rigid interconnection between tetrazoles, which in turn, along with the need to arrange the alkyl groups on tin within the lattice, dictates the build-up of either two- or three-dimensional arrays. These two classes of lattice are typified by **II**, R = Et and Bu^n, respectively.[3]

We now report on the synthesis of bis(organotin tetrazoles) linked by flexible $-(CH_2)_n-$ chains and a novel layer structure which is adopted by a representative member of the group.

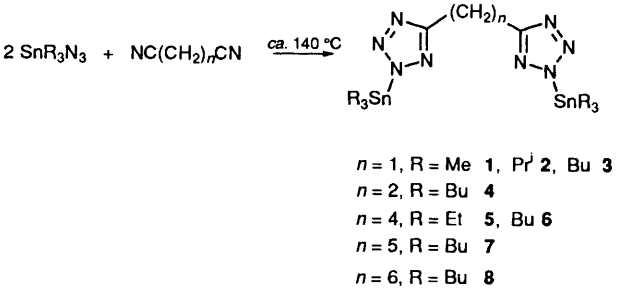

n = 1, R = Me **1**, Pr^i **2**, Bu **3**
n = 2, R = Bu **4**
n = 4, R = Et **5**, Bu **6**
n = 5, R = Bu **7**
n = 6, R = Bu **8**

Scheme 1

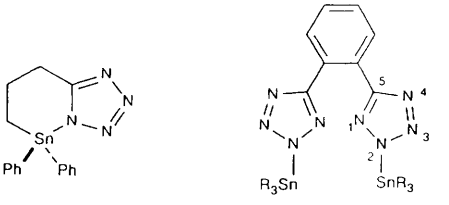

I **II**

Results and Discussion

The new bis(organotin tetrazoles) **1**–**8** have been straightforwardly synthesised by a cycloaddition reaction involving an organotin azide and an α,ω-dicyanoalkane (Scheme 1). As in our previous reports, the course of the reaction can be monitored by the disappearance of bands due to ν(N_3) and ν(CN) at *ca.* 2060 and 2250 cm^{-1}, respectively. The products are white solids, the solubility of which increases with alkane chain length; **4** proved to be effectively insoluble in even strongly co-ordinating solvents. In the solid state, the Mössbauer quadrupole splitting (q.s.) values for all eight compounds fall in a narrow range (3.56–3.78 mm s^{-1}) which is diagnostic of a *trans*-N_2SnC_3 stereochemistry about tin,[4] a situation which our work to date suggests is universal in organotin tetrazoles.[2,3] The observation of a single Sn–C stretch (ν_{asym}) in the IR spectrum of **1** (554 cm^{-1}) corroborates the planar nature of the C_3Sn moiety. For the less-soluble species **1**–**3**, NMR spectra in Me_2SO also indicate five-co-ordinate tin [^2J(SnH) = 70.0–83.8, ^1J(SnC) = 440.8–516.6 Hz; δ(^{119}Sn) = −43.8 to −52.5],[4] though it is likely that this arises from solvation given the spectral data for species soluble in less co-ordinating solvents. Compounds **5**–**8** proved sufficiently soluble in $CDCl_3$ or $CDCl_3$–MeOH mixtures to record spectra, and the tin chemical shifts are all to lower field (δ 0.0–48.0) while for **8** the measured ^1J(SnC) was 440 Hz. These data reflect the breakdown of the intermolecular Sn · · · N interactions, but some extent of oligomeric character and weak intermolecular bonding appears to be retained.

The structure of 1,6-(2-$Bu_3SnN_4C)_2(CH_2)_6$ **8** is shown in Fig. 1. Atomic coordinates are given in Table 1, selected bond lengths and angles in Table 2 while Table 3 includes data from related organotin tetrazoles. The asymmetric unit shown in Fig. 1 comprises one and a half molecular units [the second half of the hexyl chain based on C(38)–C(40) is symmetry generated], such that the total contents of the unit cell are six metals and three complete bis(tetrazole) ligands.

The *trans*-N_2SnC_3 geometry about tin suggested by the Mössbauer data is confirmed, though Sn(2) differs from Sn(1) and Sn(3) in its co-ordination. Thus, Sn(1) and Sn(3) are both co-ordinated to N^1 + N^2 sites on the tetrazoles while Sn(2) adopts an N^1 + N^1 arrangement. The Mössbauer spectrum of compound **8** fails to distinguish these different tin environments, though this is not surprising given their similar nature. In addition, while the tetrazoles based on N(1)–N(4) and N(5)–N(8) adopt an N^1 + N^3 co-ordination mode, the ring involving N(9)–N(12) bonds to tin in an N^1 + N^4 manner. In previous work we have generally observed N^1 + N^3 co-ordination for the tetrazoles, presumably as the sterically least-demanding combination of ligating atoms, in combination with N^1 + N^1 [1,2-(2-$Et_3SnN_4C)_2C_6H_4$], N^1 + N^2 [1,2-(2-$Bu_3SnN_4C)_2$-C_6H_4] and N^2 + N^2 [1,2-(2-$Et_3SnN_4C)_2C_6H_4$] bonding with respect to tin.[3] The N^1 + N^4 tetrazole co-ordination does, however, occur in **I**,[2] while N^2 + N^3 co-ordination is

typified by the tetrazoles of $[Mn_2(CO)_6(N_4CCF_3)_3]^-$.[8] All three tin centres in **8** incorporate short and long (presumably intra- and inter-molecular) Sn–N bonds [Sn(1)–N(3) 2.35(1), Sn(1)–N(9) 2.43(1); Sn(2)–N(1) 2.37(2), Sn(2)–N(5) 2.44(2); Sn(3)–N(7) 2.36(2), Sn(3)–N(12′) 2.43(2) Å], and almost identical N–Sn–N angles [175.4(5), 175.0(5), 177.6(6)° for Sn(1), Sn(2) and Sn(3), respectively]. Interestingly, the Sn(2) site, which utilises the two most sterically demanding co-ordination centres on the tetrazole (N^1), generates no more geometric distortion at tin than the $N^1 + N^2$ co-ordinated metals, contary to our observations on this matter with regard to the tin environments in 1,2-(2-$Et_3SnN_4C)_2C_6H_4$.[3]

The lattice structure of compound **8** is made up of discrete bilayers, a section of which is shown in Plate 1. Half of the hexyl groups [C(41)–C(48)] are used to join the polymer strands shown in Fig. 1 into sheets, while the other half [C(38)–C(40) and their symmetry-related partners] are used to join two centrosymmetrically related sheet structures together into a bilayer array. In Plate 1(*a*) the atoms are colour coded to show members of unique sheet structures, while the interlayer hexyl units are also highlighted. Each sheet incorporates large, 40-atom rings of empirical formula $C_{18}N_{16}Sn_6$ which are relatively

Table 1 Fractional atomic coordinates (× 10^4) for compound **8**

Atom	*x*	*y*	*z*
Sn(1)	5054(1)	5233(1)	3301(1)
Sn(2)	2351(1)	1441(1)	3050(1)
Sn(3)	−722(1)	−2055(1)	2943(1)
N(1)	2765(10)	3029(9)	3377(9)
N(2)	3670(10)	3350(10)	3259(10)
N(3)	3715(10)	4242(9)	3452(10)
N(4)	2907(10)	4507(8)	3715(9)
N(5)	1777(11)	−173(9)	2637(10)
N(6)	1061(10)	−434(9)	3014(10)
N(7)	696(11)	−1267(10)	2658(11)
N(8)	1186(12)	−1581(10)	2059(11)
N(9)	6487(11)	6287(9)	3270(11)
N(10)	7241(11)	6391(10)	3995(10)
N(11)	8047(11)	6872(10)	3954(12)
N(12)	−2190(10)	−2908(9)	3179(11)
C(37)	2313(12)	3744(11)	3674(11)
C(38)	1293(12)	3717(11)	3948(14)
C(39)	1101(12)	4628(11)	4468(13)
C(40)	86(12)	4544(11)	4732(13)
C(41)	1840(12)	−892(12)	2051(11)
C(42)	2524(14)	−935(13)	1437(13)
C(43)	3271(14)	−1659(13)	1546(12)
C(44)	4030(18)	−1664(16)	995(16)
C(45)	4745(16)	−2429(15)	1038(13)
C(46)	5464(14)	−2420(12)	1942(14)
C(47)	6244(13)	−3132(12)	1877(12)
C(48)	6819(13)	6747(11)	2760(13)

Table 2 Selected bond distances (Å) and angles (°) for compound **8**

C(1)–Sn(1)	2.14(2)	C(5)–Sn(1)	2.19(2)
C(9)–Sn(1)	2.19(3)	N(3)–Sn(1)	2.35(1)
N(9)–Sn(1)	2.43(1)	C(13)–Sn(2)	2.11(2)
C(17)–Sn(2)	2.14(2)	C(21)–Sn(2)	2.13(2)
N(1)–Sn(2)	2.37(2)	N(5)–Sn(2)	2.44(2)
C(25)–Sn(3)	2.27(3)	C(26)–Sn(3)	2.89(4)
C(29)–Sn(3)	2.34(4)	C(30)–Sn(3)	2.74(4)
C(33)–Sn(3)	2.16(3)	N(7)–Sn(3)	2.36(2)
N(12′)–Sn(3)	2.43(2)		
C(5)–Sn(1)–C(1)	118.8(9)	C(9)–Sn(1)–C(1)	122.8(10)
C(9)–Sn(1)–C(5)	118.2(10)	N(3)–Sn(1)–C(1)	87.6(8)
N(3)–Sn(1)–C(5)	90.5(8)	N(3)–Sn(1)–C(9)	87.9(9)
N(9)–Sn(1)–C(1)	88.6(8)	N(9)–Sn(1)–C(5)	89.2(7)
N(9)–Sn(1)–C(9)	96.3(9)	N(9)–Sn(1)–N(3)	175.4(5)
C(17)–Sn(2)–C(13)	111.2(7)	C(21)–Sn(2)–C(13)	123.6(9)
C(21)–Sn(2)–C(17)	124.8(9)	N(1)–Sn(2)–C(13)	93.3(7)
N(1)–Sn(2)–C(17)	90.7(7)	N(1)–Sn(2)–C(21)	92.3(8)
N(5)–Sn(2)–C(13)	88.8(7)	N(5)–Sn(2)–C(17)	92.7(7)
N(5)–Sn(2)–C(21)	82.8(8)	N(5)–Sn(2)–N(1)	175.0(5)
C(29)–Sn(3)–C(25)	146.8(12)	C(33)–Sn(3)–C(25)	98.9(12)
C(33)–Sn(3)–C(29)	114.2(13)	N(7)–Sn(3)–C(25)	89.1(10)
N(7)–Sn(3)–C(29)	92.5(13)	N(12′)–Sn(3)–C(29)	85.2(13)
N(7)–Sn(3)–C(33)	88.7(11)	N(12′)–Sn(3)–C(25)	93.2(10)
N(12′)–Sn(3)–C(30)	87.3(11)	N(12′)–Sn(3)–N(7)	177.6(6)

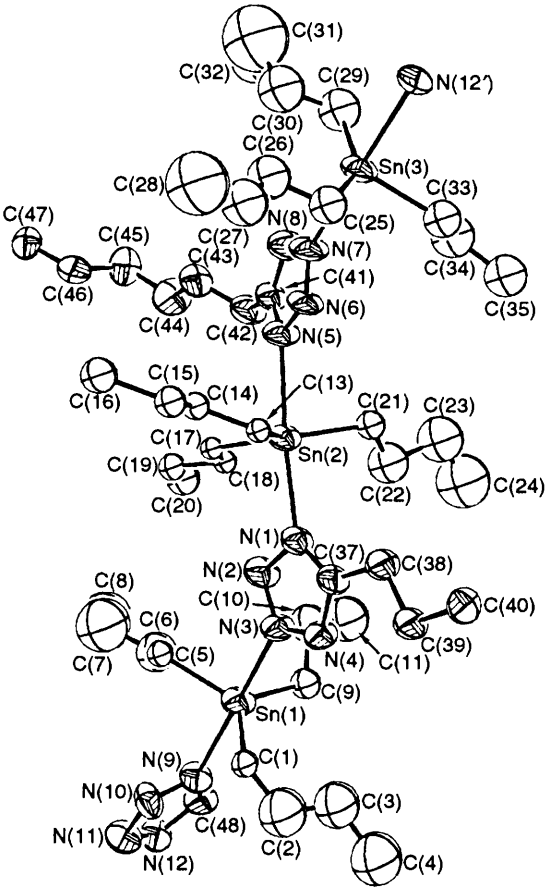

Fig. 1 The asymmetric unit (comprising one and a half molecular units) of compound **8** showing the labelling scheme used. Atom C(12), one of the γ-carbons bonded to Sn(1), was not located due to disorder

Table 3 Comparative geometric data for compound **8** and related species

Compound	Co-ordination number	*d*(Sn–N)/Å		N–Sn–N/°	Ref.
		Intramolecular	Intermolecular		
8	5	2.35(2)–2.37(2)	2.43(1)–2.44(2)	175.0(5)–177.6(6)	This work
1,3-(2-$Bu_3SnN_4C)_2C_6H_4$·2MeOH	5	2.28(1), 2.27(1)	—	176.6(3)	3
1,2-(2-$Et_3SnN_4C)_2C_6H_4$	5	2.354(6), 2.364(6)	2.553(7), 2.415(9)	167.8(1), 175.0(3)	3
1,2-(2-$Bu_3SnN_4C)_2C_6H_4$	5	2.24(5)–2.42(5)	2.44(7)–2.47(6)	174(2)–179(2)	3
$Ph_2Sn(CH_2)_3CN_4$ **I**	5	2.339	2.371	173.8(5), 174.1(5)	2
$SnMe_3N_3$	5	2.390	2.390		5
$SnMe_3N_3$·$SnMe_3(OH)$	5	2.442	2.612		6
$[\{Fe(CO)_2(\eta\text{-}C_5H_5)\}_2Sn(N_3)_2]$	4	2.158	—		7

planar and rectangular in nature. These rings can be seen in Plate 1(*a*) as, for example, the red parallel chains containing Sn(3), Sn(2), Sn(1) and Sn(2), Sn(1), Sn(3) linked by hexyl groups of the same colour. This ring is *ca.* 19.6 Å long (distance between common atoms in the hexyl chains) and its maximum and minimum widths can be estimated as 11.4 [Sn(1) · · · Sn(2)] and 8.7 Å [Sn(1) · · · Sn(3)], respectively. These cavities are, as with previous porous organotin tetrazole structures we have reported, filled by the alkyl groups on tin, which are thus fundamentally implicated in generating the overall lattice design. A similar comment can be made with respect to the other macrocyles which can be identified within the supramolecular array of **8** (see below). The view of the lattice along *c* [Plate 1(*b*)] can be realised by eclipsing the two sheets shown in Plate 1(*a*). This view highlights the square channels running through the lattice as bilayer units are stacked on top of each other.

Plate 1(*c*) is the first of two orthogonal views of the bilayer (along *a*), and reveals the non-planar nature of the layer structure and also illustrates the formation of hexagonal-looking channels within the bilayer. The separation between individual bilayers is difficult to quantify due to the non-planar nature of the layers, but is *ca.* 8 Å [Sn(2) · · · C(42) 8.4 Å]. The origin of the hexagonal channels is shown in Plate 1(*a*) as parallel sections of blue and red chains (*i.e.* in different halves of the bilayer) linked by green hexyl groups. These have the same 40-atom empirical formula ($C_{18}N_{16}Sn_6$) which makes up the more rectangular channels described above. The lengths of these two empirically related rings are essentially the same (19.6 Å), though the latter rings are somewhat wider in general [Sn(1) · · · Sn(2) 13.4, Sn(3) · · · Sn(3) 15.5 Å]. When the layers are viewed along *b* [Plate 1(*d*)] further highly elliptical channels can be identified, the composition of which is shown more clearly in Plate 1(*a*) as the shaded atoms which form a 'step-like' arrangement within the bilayer. These 58-atom rings of formula $C_{34}N_{18}Sn_6$ are the largest within the lattice, with estimated dimensions of 25.5 [C(47) · · · C(47)] × 5.8 Å [Sn(1) · · · Sn(1)]. It is noteworthy that the three channel types are remarkably different despite the fact that each contains six organotin units. Moreover, all of the cavities within compound **8** are larger than the 24-atom, tetranuclear $C_8N_{12}Sn_4$ units which we previously observed as being central to the structure of 1,2-(2-Et_3SnN_4C)$_2C_6H_4$.[3]

In summary, the structure of 1,6-(2-Bu_3SnN_4C)$_2(CH_2)_6$ reveals yet another variety of supramolecular array and underlines the diversity of structures adopted by this family of organotins.

Experimental

Spectra were recorded on the following instruments: JEOL GX270 (^{1}H, ^{13}C NMR), GX60Q and GX400 (^{119}Sn NMR), Perkin-Elmer 599B (IR). Details of our Mössbauer spectrometer and related procedures are given elsewhere.[9] Triorganotin azides SnR_3N_3 were prepared by literature methods (R = Me,[10] Et[3] or Bu[11]) and employed without further purification. All nitriles and other reagents were of commercial origin (*e.g.* Aldrich) used without further purification. **CAUTION**: owing to their potentially explosive nature, all preparations of and subsequent reactions with organotin azides were conducted under an inert atmosphere behind a rigid safety screen.

Syntheses

Bis(2-trimethylstannyltetrazol-5-yl)methane 1. Malononitrile (0.58 g, 0.8 mmol) and trimethyltin azide (3.5 g, 1.6 mmol) were heated under nitrogen in a small round-bottomed flask at 140 °C for 30 min. This resulted in a slightly charred grey mass which was dissolved in boiling methanol and decolourised with activated charcoal. Hot filtration followed by *in vacuo* removal of solvent yielded an off-white gum which was extracted with methanol in a Soxhlet apparatus and reprecipitated as an amorphous solid (1.8 g, 44%), m.p. > 240 °C [Found (Calc. for $C_9H_{20}N_8Sn_2$): C, 23.1 (22.6); H, 4.20 (4.20); N, 22.9 (23.4)%]. NMR [$(CD_3)_2SO$]: ^{1}H, δ 0.57 (s, 18 H, CH_3), 4.26 (s, 2 H, CH_2); ^2J(C^1H_3–^{117,119}Sn) 70.0 Hz (unresolved); ^{13}C, δ −0.4 (CH_3), 21.6 (CH_2) and 158.77 (CN_4); ^1J($^{13}CH_3$–^{117,119}Sn) 516.6 Hz (unresolved); ^{119}Sn, δ −43.8. ^{119}Sn Mössbauer (mm s^{-1}): i.s. = 1.40, q.s. = 3.57. IR (cm^{-1}, KBr disc): 3002, 2921, 1483, 1414, 1375, 1221, 1096, 787, 761, 662 and 554.

The following compounds were prepared by the same general procedure.

Bis(2-triisopropylstannyltetrazol-5-yl)methane 2. Yield = 22%, m.p. 190 °C (decomp.) [Found (Calc. for $C_{21}H_{44}N_8Sn_2$): C, 38.9 (39.0); H, 6.80 (6.85); N, 16.9 (16.9)%]. NMR [$(CD_3)_2SO$]: ^{1}H, δ 1.23 [s, 18 H, $(CH_3)_2CH$], 1.92 [m, 3 H, $(CH_3)_2CH$] and 4.31 (s, 2 H, CH_2); ^3J[$(C^1H_3)_2CH$–^{117,119}Sn] 79.0, 83.8 Hz; ^{13}C, δ 21.1 [$(CH_3)_2CH$], 24.2 [$(CH_3)_2CH$], 24.2 (CH_2) and 162.6 (CN_4); ^1J[$(CH_3)_2{}^{13}CH$–^{117,119}Sn] 440.8 (unresolved); ^2J[$(^{13}CH_3)_2CH$–^{117,119}Sn] 19.8 Hz (unresolved); ^{119}Sn, δ −84.1. ^{119}Sn Mössbauer (mm s^{-1}): i.s. = 1.52, q.s. = 3.68. IR (cm^{-1}, KBr disc): 2963, 2936, 2861, 1464, 1385, 1367, 1273, 1224, 1206, 1156, 1109, 1088, 1006, 619 and 478.

Bis(2-tributylstannyltetrazol-5-yl)methane 3. Yield = 45%, m.p. 209–212 °C (decomp.) [Found (Calc. for $C_{27}H_{56}N_8Sn_2$): C, 44.7 (44.6); H, 8.00 (7.75); N, 15.5 (15.4)%]. NMR [$(CD_3)_2SO$]: ^{1}H, δ 0.93 [t, 18 H, $(CH_2)_3CH_3$], 1.12 [t, 12 H, $SnCH_2(CH_2)_2CH_3$], 1.40 [m, 12 H, $Sn(CH_2)_2CH_2CH_3$], 1.65 [m, 12 H, $CH_2CH_2CH_2CH_3$] and 3.30 (s, 2 H, CH_2); ^{13}C, δ 13.6 [$(CH_2)_3CH_3$], 18.2 [$SnCH_2(CH_2)_2CH_3$], 22.8 (CH_2), 26.4 [$Sn(CH_2)_2CH_2CH_3$], 27.7 [$SnCH_2CH_2CH_2CH_3$] and 160.0 (CN_4); ^{119}Sn, δ −52.5. ^{119}Sn Mössbauer (mm s^{-1}): i.s. = 1.47, q.s. = 3.59. IR (cm^{-1}, KBr disc): 2959, 2924, 2872, 2857, 1487, 1464, 1397, 1377, 1082, 879, 698, 680, 613 and 509.

1,2-Bis(2-tributylstannyltetrazol-5-yl)ethane 4. Yield = 65%, m.p. 218 °C (decomp.). The compound was too insoluble for solution-state NMR spectra [Found (Calc. for $C_{28}H_{58}N_8Sn_2$): C, 45.3 (45.1); H, 7.95 (7.80); N, 15.2 (15.1)%]. ^{119}Sn Mössbauer (mm s^{-1}): i.s. = 1.38, q.s. = 3.78. IR (cm^{-1}, KBr disc): 2955, 2924, 2869, 1476, 1391, 1262, 1227, 1130, 1080, 1022, 870, 803, 706, 679 and 615.

1,4-Bis(2-triethylstannyltetrazol-5-yl)butane 5. Yield = 62%, m.p. 195 °C (decomp.) [Found (Calc. for $C_{18}H_{38}N_8Sn_2$): C, 37.0 (35.8); H, 6.40 (6.30); N, 17.2 (18.6)%]. NMR: ^{1}H ($CDCl_3$), δ 0.92 (t, 18 H, CH_3), 2.12 (m, 12 H, $SnCH_2CH_3$) and 3.62 (m, butane protons); ^{13}C (MeOH–$CDCl_3$), δ 7.1 (CH_3), 8.5 ($SnCH_2CH_3$), 25.2 [$CH_2(CH_2)_2CH_2$] and 28.3 [$CH_2(CH_2)_2CH_2$]; ^{119}Sn ($CDCl_3$), δ 15.8. ^{119}Sn Mössbauer (mm s^{-1}): i.s. = 1.44, q.s. = 3.56.

1,4-Bis(2-tributylstannyltetrazol-5-yl)butane 6. Yield = 58%, m.p. 133 °C [Found (Calc. for $C_{30}H_{62}N_8Sn_2$): C, 46.3 (46.9); H, 8.20 (8.05); N, 14.6 (14.6)%]. NMR: ^{1}H ($CDCl_3$), δ 0.90 (t, 18 H, CH_3), 1.32 (m, 24 H, $SnCH_2CH_2CH_2CH_3$), 1.55 (m, 12 H, $SnCH_2CH_2CH_2CH_3$) and 3.60 [m, 8 H, $(CH_2)_4$]; ^{13}C (MeOH–$CDCl_3$), δ 12.2 (CH_3), 15.5 [$SnCH_2(CH_2)_2CH_3$], 23.5 ($CH_2CH_2CH_2CH_2$), 26.0 ($SnCH_2CH_2CH_2CH_3$), 27.0 ($CH_2CH_2CH_2CH_2$), 27.2 ($SnCH_2CH_2CH_2CH_3$) and 178.0 (CN_4); ^3J($CH_2CH_2{}^{13}CH_2CH_2CH_3$–^{117,119}Sn) 74.0 Hz (unresolved); ^{119}Sn ($CDCl_3$), δ 48.0. ^{119}Sn Mössbauer (mm s^{-1}): i.s. = 1.47, q.s. = 3.67.

1,5-Bis(2-tributylstannyltetrazol-5-yl)pentane 7. Yield = 34%, m.p. 130 °C [Found (Calc. for $C_{31}H_{64}N_8Sn_2$): C, 47.4 (47.3); H, 8.25 (8.20); N, 14.2 (14.3)%]. NMR: ^{1}H ($CDCl_3$), δ 0.90 (t, 18 H, CH_3), 1.25 (m, 24 H, $SnCH_2CH_2CH_2CH_3$), 1.59 (m, 12 H, $SnCH_2CH_2CH_2CH_3$) and 2.21 [m, 10 H, $(CH_2)_5$];

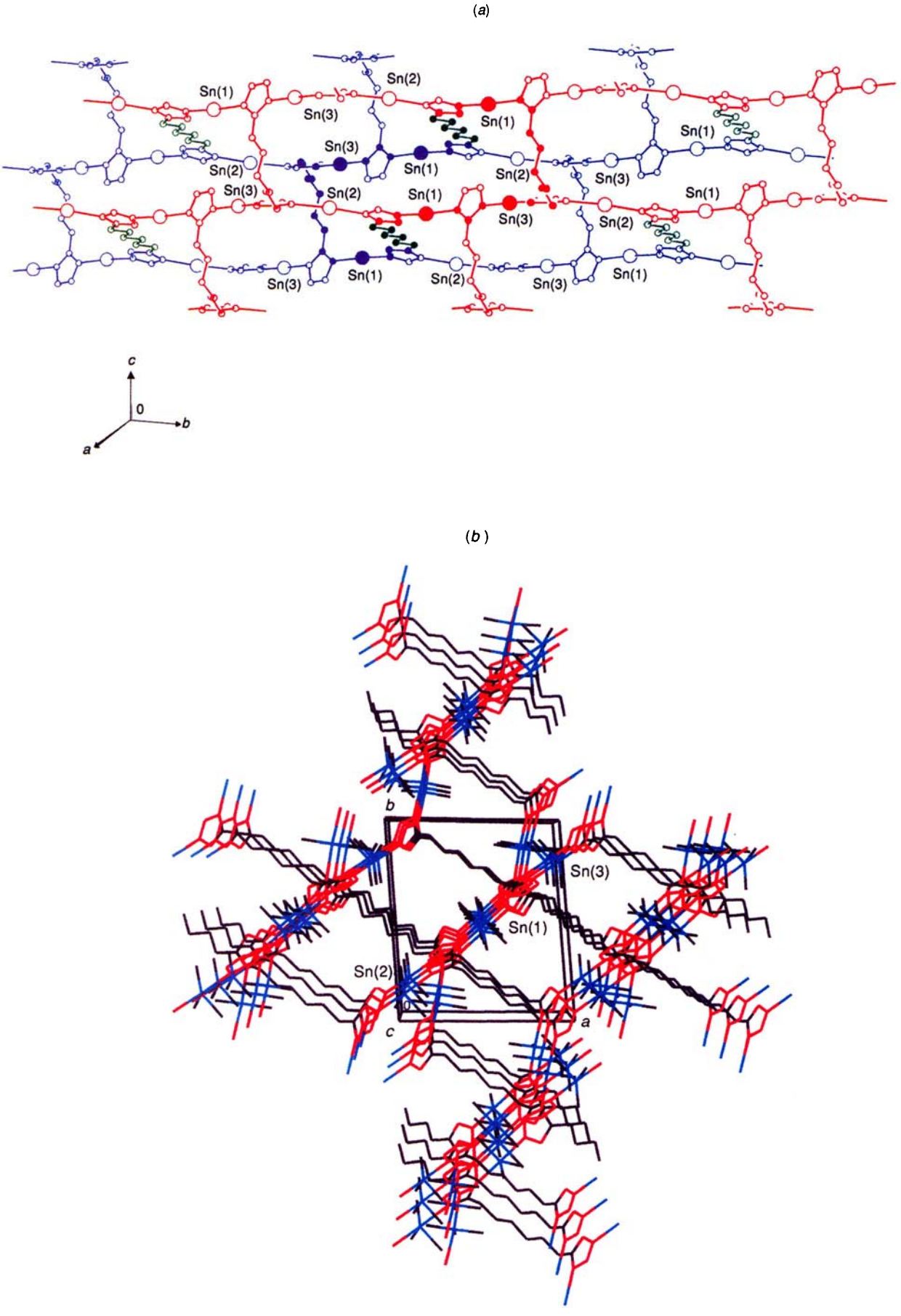

Plate 1 (*a*) The bilayer nature of compound **8**. Only the α-carbon atoms of the *n*-butyl groups are shown for clarity. Atoms coloured red and blue belong to separate layers and are linked into the bilayer arrangement by the hexyl groups (green). Shaded atoms refer to the channels shown in Plate 1(*d*) (see text). (*b*) View of the unit cell perpendicular to *ab* showing the channels generated by stacking of the layers in (*a*)

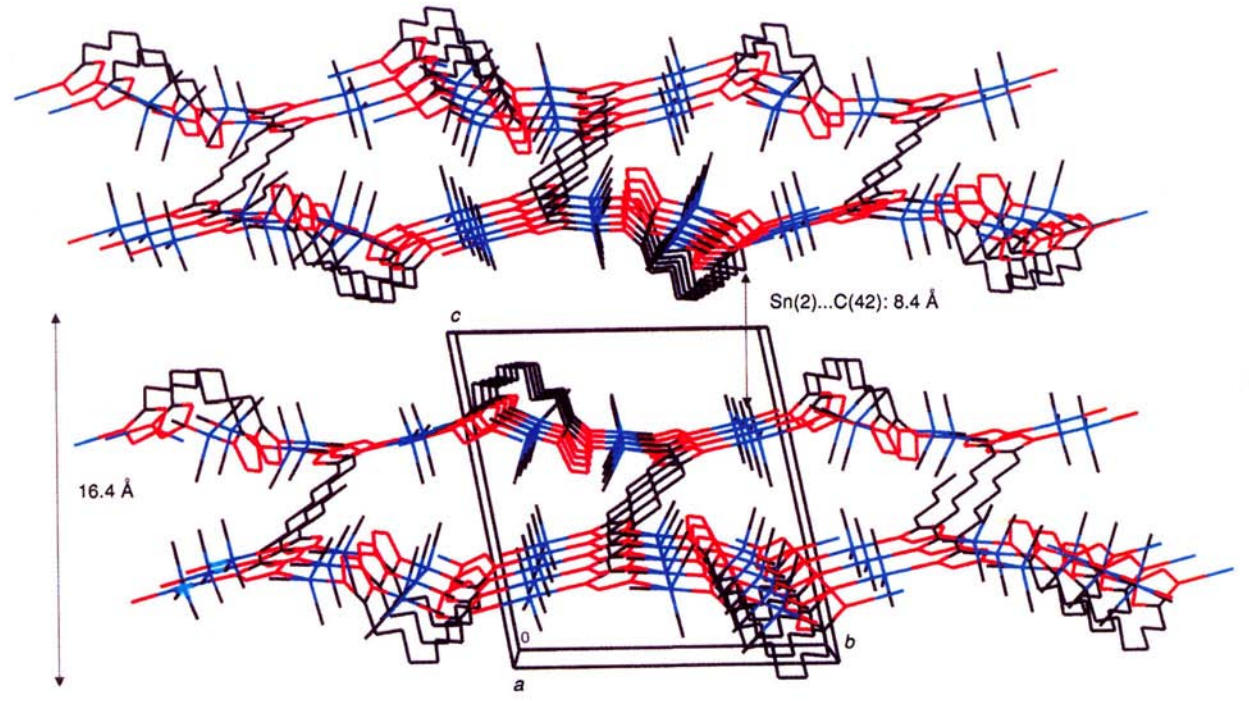

(*d*)

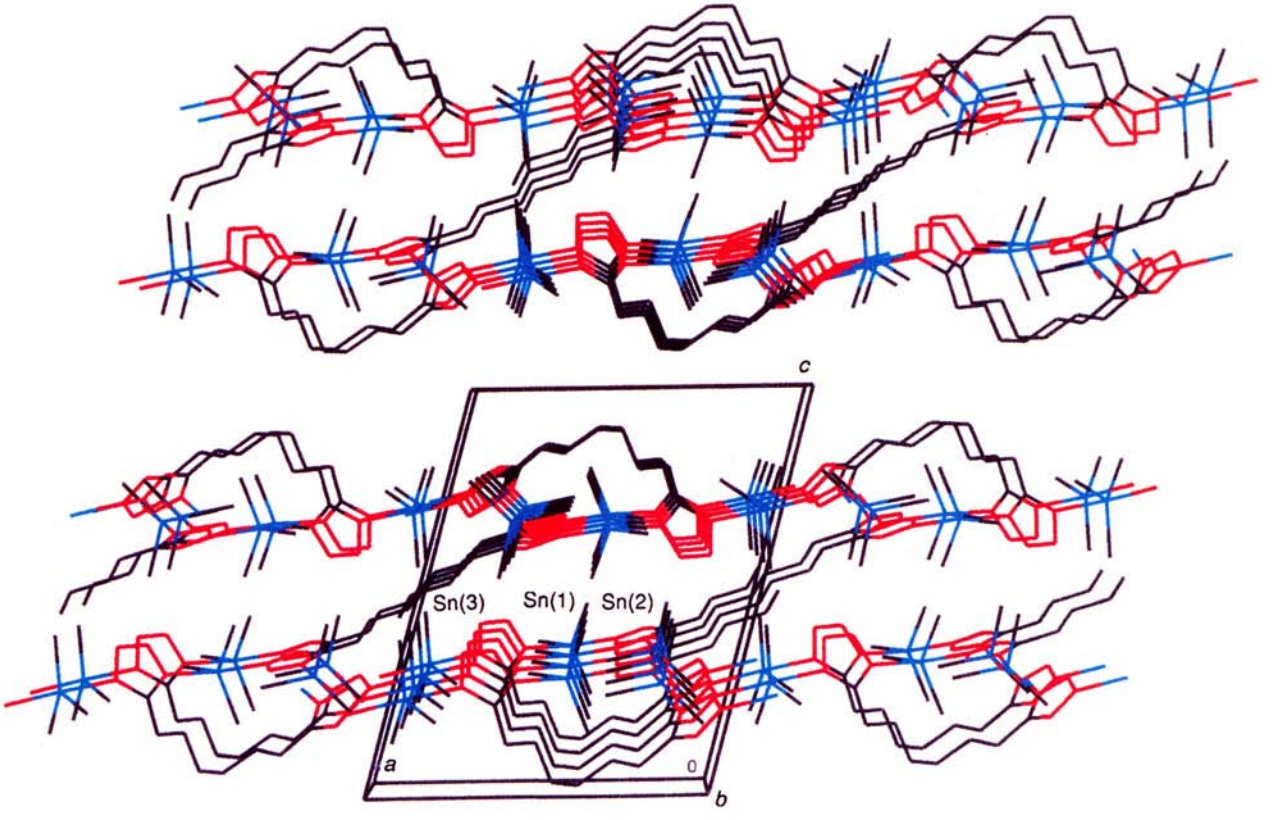

Plate 1 (*c*) View orthogonal to the bilayer (along *a*) which shows the formation of hexagonal channels. (*d*) View of the lattice along *b* showing elliptical channel formation

^{13}C (MeOH–$CDCl_3$), δ 12.5 (CH_3), 17.0 [$SnCH_2(CH_2)_2CH_3$], 23.6 [$(CH_2)_2CH_2(CH_2)_2$], 25.2 ($CH_2CH_2CH_2CH_2CH_2$), 25.4 [$Sn(CH_2)_2CH_2CH_3$], 26.9 [$CH_2(CH_2)_3CH_2$], 27.5 ($SnCH_2$-$CH_2CH_2CH_3$) and 174.0 (CN_4); $^3J(CH_2CH_2{}^{13}CH_2$-$CH_3{}^{-117,119}Sn)$ 72.0 Hz (unresolved); ^{119}Sn ($CDCl_3$), δ 0.0. ^{119}Sn Mössbauer (mm s^{-1}): i.s. = 1.46, q.s. = 3.62.

1,6-Bis(2-tributylstannyltetrazol-5-yl)hexane 8. Yield = 13% [Found (Calc. for $C_{32}H_{66}N_8Sn_2$): C, 48.1 (48.0); H, 8.85 (8.25); N, 12.1 (14.0)%]. NMR: ^1H ($CDCl_3$), δ 0.88 (t, 18 H, CH_3), 1.25 (m, 24 H, $SnCH_2CH_2CH_2CH_3$), 1.47 (m, 12 H, $SnCH_2$-$CH_2CH_2CH_3$) and 2.10 [m, 12 H, $(CH_2)_6$]; ^{13}C (MeOH–$CDCl_3$), δ 12.4 (CH_3), 16.5 [$SnCH_2(CH_2)_2CH_3$], 23.5 [$(CH_2)_2(CH_2)_2(CH_2)_2$], 26.1 [$Sn(CH_2)_2CH_2CH_3$], 26.9 [CH_2-$CH_2(CH_2)_2CH_2CH_2$], 27.1 ($SnCH_2CH_2CH_2CH_3$), 27.6 [CH_2-$(CH_2)_4CH_2$] and 162.0 (CN_4); $^1J[^{13}CH_2(CH_2)_2CH_3$-$^{117,119}Sn]$ 413, 440; $^2J[CH_2{}^{13}CH_2CH_2CH_3{}^{-117,119}Sn]$ 27 (unresolved); $^3J[(CH_2)_2{}^{13}CH_2CH_3{}^{-117,119}Sn]$ 77 Hz (unresolved); ^{119}Sn ($CDCl_3$), δ 20.0. ^{119}Sn Mössbauer (mm s^{-1}): i.s. = 1.44, q.s. = 3.61.

X-Ray crystallography

A crystal of compound **8** of approximate dimensions 0.2 × 0.2 × 0.15 mm was used for data collection.

Crystal data. $C_{48}H_{99}N_{12}Sn_3$, M = 1200.5, triclinic, space group $P\bar{1}$ (no. 2), a = 13.154(3), b = 15.041(5), c = 16.444(3) Å, α = 100.07(2), β = 104.43(2), γ = 92.21(2)°, U = 3090.7 $Å^3$, Z = 2, D_c = 1.29 g cm^{-3}, μ(Mo-Kα) = 12.4 cm^{-1}, $F(000)$ = 1242.

Data were measured at room temperature on a CAD4 automatic four-circle diffractometer in the range $2 \leqslant \theta \leqslant 24°$. 10 066 Reflections were collected of which 4678 were unique with $I \geqslant 2\sigma(I)$. Data were corrected for Lorentz and polarisation effects but not for absorption. As the crystal was not a strong diffractor the scan time was increased during data collection and the $\sigma(I)/I$ parameter was also varied to minimise the number of reflections which would be flagged as weak. This threshold adjustment was effected to improve the quality and confidence in relatively weak data. The structure was solved by direct methods and refined using the SHELX [12,13] suite of programs. In the final least-squares cycles the tin and nitrogen atoms along with carbons C(37)–C(48) were allowed to vibrate anisotropically. The butyl carbons [which were all located except for C(12)] were treated isotropically. Refinement was assisted considerably by fixing the bond distances in five alkyl groups [C(5)–C(8), C(9)–C(11), C(21)–C(24), C(29)–C(32) and C(33)–C(36)] where shift/e.s.d. values would have otherwise remained high. Hydrogen atoms were included at calculated positions except on C(11) [due to smearing in the C(12) position] and C(40) (which is close to an inversion centre). Final residuals (refinement based on F) after 14 cycles of least squares were R = 0.0790, R' = 0.0866, for a weighting scheme w = $1.9870/[\sigma^2(F) + 0.003\,578(F)^2]$. Maximum final shift/e.s.d. was 0.060. The maximum and minimum residual densities were 0.67 and −0.32 e $Å^{-3}$, respectively.

Complete atomic coordinates, thermal parameters and bond lengths and angles have been deposited at the Cambridge Crystallographic Data Centre. See Instructions for Authors, *J. Chem. Soc., Dalton Trans.*, 1996, Issue 1.

Acknowledgements

We thank the SERC (now EPSRC) for financial support and a studentship (to M. H.).

References

1 M. F. Mahon, K. C. Molloy and P. C. Waterfield, *J. Organomet. Chem.*, 1989, **361**, C5.
2 S. J. Blunden, M. F. Mahon, K. C. Molloy and P. C. Waterfield, *J. Chem. Soc., Dalton Trans.*, 1994, 2135.
3 M. Hill, M. F. Mahon, J. McGinley and K. C. Molloy, preceding paper.
4 A. G. Davies and P. J. Smith, in *Comprehensive Organometallic Chemistry*, eds. G. Wilkinson, F. G. A. Stone and E. W. Abel, Pergamon, Oxford, 1982, p. 529.
5 R. Allman, R. Hohlfeld, A. Waskowska and J. Lörberth, *J. Organomet. Chem.*, 1980, **192**, 353.
6 R. Allman, R. Hohlfeld, S. Olejnik and J. Lörberth, *J. Organomet. Chem.*, 1981, **210**, 51.
7 M. J. Hampden-Smith, D. Lei and E. N. Duesler, *J. Chem. Soc., Dalton Trans.*, 1990, 2953.
8 E. O. John, R. D. Willet, B. Scott, R. L. Kirchmeir and J. M. Shreeve, *Inorg. Chem.*, 1989, **28**, 893.
9 K. C. Molloy, T. G. Purcell, K. Quill and I. W. Nowell, *J. Organomet. Chem.*, 1984, **267**, 237.
10 J. S. Thayer and R. West, *Inorg. Chem.*, 1964, **3**, 889.
11 W. T. Reichle, *Inorg. Chem.*, 1964, **3**, 402.
12 G. M. Sheldrick, SHELX 76, A program for crystal structure determination, University of Cambridge, 1976.
13 G. M. Sheldrick, SHELXS 86, A program for crystal structure determination, University of Göttingen, 1986.

Received 22*nd August* 1995; *Paper* 5/05578D